Recent results in Silicon Photonics at the University of Southampton

G T Reed, G Z Mashanovich, F Y Gardes, D J Thomson, Y Hu, J Soler-Penades , M Nedeljkovic, A Z Khokhar, P Thomas, C Littlejohns, A Ahmad, S Reynolds, R Topley, C Mitchell, S Stankovic, N Owens , X Chen

Optoelectronics Research Centre, University of Southampton, Southampton, Hampshire, SO17 1BJ, UK

P R Wilson, L Ke, T M Ben Masaud, A Tarazona, H Chong

School of Electronics and Computer Sciences, University of Southampton, Southampton, Hampshire, SO17 1BJ, UK

ABSTRACT

In this paper we will discuss recent results in our work on Silicon Photonics. This will include active and passive devices for a range of applications. Specifically we will include work on modulators and drivers, deposited waveguides, multiplexers, device integration and Mid IR silicon photonics. These devices and technologies are important both for established applications such as integrated transceivers for short reach interconnect, as well as emerging applications such as disposable sensors and mass market photonics.

INTRODUCTION

Silicon Photonics has been seen as the primary candidate for short-reach interconnect for several years, and additional applications continue to emerge such as Mid IR sensor circuits, Fibre to the Home, and even interconnect for consumer devices. For this variety of applications, flexible devices are required that can be optimised for a given application. Therefore we have been developing a library of components that include both active and passive devices for a range of wavelengths. Some of the recently developed devices are discussed in this paper.

OPTICAL PHASE MODULATORS

We have developed several device variants based on two primary phase modulator designs. Both designs are based upon self-aligned processes [1-2] to simplify fabrication and provide the potential for a reliable performance, high yield and low cost production. The self-aligned process works by using the same silicon dioxide layer as the hard mask through which to etch the optical rib waveguides to also guide the n-type implant. The first design, shown in figure 1(a), is based in SOI with a 220nm thick overlayer. The rib section of the waveguide (220nm x 400nm) and slab (100nm thick) to one side is doped p type (3e17.cm-3) and the slab to the other side doped n type (1.5e18.cm-3). The second design is shown in figure 1(b). This version is based in 400nm thick overlayer SOI. The waveguides fabricated can support the propagation of both fundamental TE and TM modes. Depletion is achieved at a pn junction that is wrapped around the top and two sides of the waveguide as shown in figure 1(b). The purpose of this design is to achieve polarisation independent modulation. This can be obtained by tailoring the position of the doped regions and the density of active dopants within them to match the modulation efficiency for the TE and TM polarisation modes. The p and n type regions are both doped to a level of ~1e18.cm-3. Operation at 10Gbit/s and 40Gbit/s with the same extinction ratio (6.5dB) for both TE and TM polarisations is demonstrated [2].

The phase modulator of figure 1(a) has been incorporated into both MZI modulators [1], ring resonators [3], slow wave modulators [4-6], modulated via simple on-off keying up to 50Gb/s [7], or DPSK up to 20Gb/s [8]. We have also

Smart Photonic and Optoelectronic Integrated Circuits XVI, edited by Louay A. Eldada, El-Hang Lee, Sailing He, Proc. of SPIE Vol. 8989, 89890D · © 2014 SPIE · CCC code: 0277-786X/14/$18
doi: 10.1117/12.2045490

integrated the devices with other components such as modulator drivers in wire bonded configurations [9], or front end integration [10], as well as with other optical components (e.g. sources[11]).

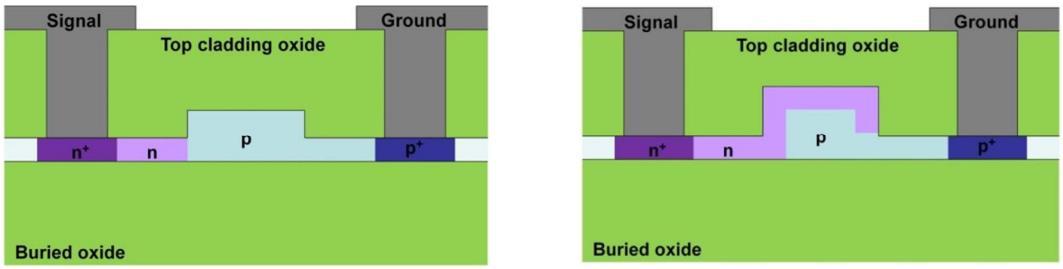

(a) (b)

Fig. 1. Cross sectional diagram of the two modulator designs (a) 220nm carrier depletion phase modulator and (b) 400nm carrier depletion phase modulator.

ANGLED MMI MULTIPLEXERS

We have developed novel coarse multiplexer structures based upon angled MMIs (AMMI) the basic structure of which is shown schematically in figure 2. The input waveguide accesses the multimode dispersion waveguide on one side wall at a tilt angle of θ_t. The output waveguides access the multimode dispersion waveguide on the other side wall at the same tilt angle, whilst the axial distance between the access point of the input waveguide and that of the ith output waveguide, L_i, is determined by the self-imaging condition of an MMI which is dependent on the waveguide of the light. The result is that as the position of the output waveguide is moved along the multimode dispersion waveguide the wavelength of light which exits that waveguide changes and therefore a multiplexing action is achieved. There are a few advantage of this structure over previously demonsrated multiplexing devices.

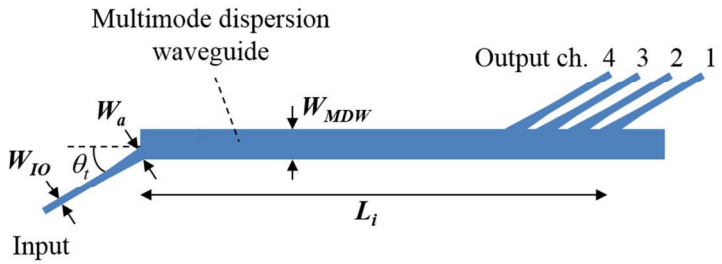

Fig. 2. Schematic design of a 4-channel AMMI

Firstly, a very low insertion loss is achievable in an AMMI since the structure is mostly composed of a large-dimensional straight multimode waveguide and therefore loss due to bends and interaction with sidewall roughness is low. Secondly, the spectral response of an AMMI structure is more tolerant to waveguide dimension errors than conventional planar waveguide WDMs, such as arrayed waveguide gratings (AWG), Mach-Zehnder interferometers (MZI) and ring resonators (RR), where the dispersive structures are based on single-mode waveguides. Thirdly, the AMMI structure benefits from ease of fabrication which is not the case with the design of SOI based low-loss AWGs or Echelle gratings [12-13], which require an additional shallow etching step at the interfaces between input/output waveguides and free propagation region for the reduction of losses due to waveguide mode mismatch. The AMMI's waveguide mode mismatch at those interfaces is low due to the wide input/output waveguides; hence, the whole structure can be

fabricated using a single lithography step and and a single etching step and the requirement of alignment between multiple lithography steps is removed.

To date we have demonstrated a 4-channel device in 400nm overlayer SOI for which the spectral response in shown in figure 3. An insertion loss of < 1 dB, a crosstalk of < -23 dB and a non-uniformity of < 0.5 dB across all the 4 channels is demonstrated. The length of the multimode region in this case is approximately 5mm. However since the width is only 25um the footprint consumed is comparable to other multiplexing sturctures. The aspect ratio of the structure is also not problematic as Mach-Zehnder modulators also have a similar length therefore the AMMI can positioned alongside them with little impact on the overall chip size. Furthermore, the length of the AMMI can be significantly reduced, although the channel spacing will be increased as a result [14].

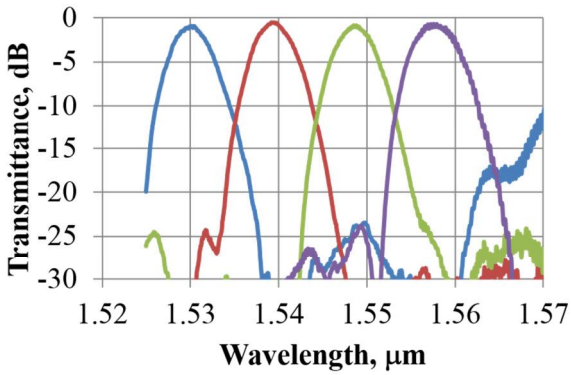

Fig. 3. Measured spectral responses of an optimized 4-channel AMMI with ~5mm long multimode region.

The number of channels can be increased by reducing the width and spacing of the output ports, however, this will impact the optical loss and crosstalk significantly [14]. An alternative approach to increasing the channel count which we have demonstrated involves using an imblanced MZI to interleave two AMMI sturctures each having 4 channels . An insertion loss of 3-4 dB and a crosstalk of –(15-20) dB was achieved across 8 channels [15]. A large proportion of the insertion loss can be attributed to the small bend radius used in the MZI structure and therefore the overall insertion loss can be improved in future iterations.

ERASABLE GRATING COUPLERS FOR WAFER-SCALE TESTING

A critical component of any large scale manufacturing line is thorough autonomous testing; this is currently not possible in photonics platforms due to the fact that light cannot be coupled into a photonic circuit at arbitrary positions in that circuit in order to test individual photonic components. Surface grating couplers can couple light from an optical fibre to a silicon waveguide but these gratings are permanent features of the surface topology, so if they are positioned throughout the circuit for testing purposes, they will permanently alter the circuit performance in an unacceptable way. Consequently, what is required is a means of accessing the photonic device via test points, but for that test point to be subsequently removed to leave the circuit unaffected. In all proposed photonic wafer scale testing systems reported to date, permanent gratings have been utilised (e.g. [16]), or gratings have been fabricated on the end of an optical fibre [17] in order to introduce a temporary coupling mechanism. We have developed a means of introducing a temporary grating coupler that can subsequently be erased, once testing is complete. An example wafer scale testing configuration is depicted schematically in figure 4. In this example configuration, a broad band input coupler is used, and several narrow band output couplers are used in order to test successively more complex circuits.

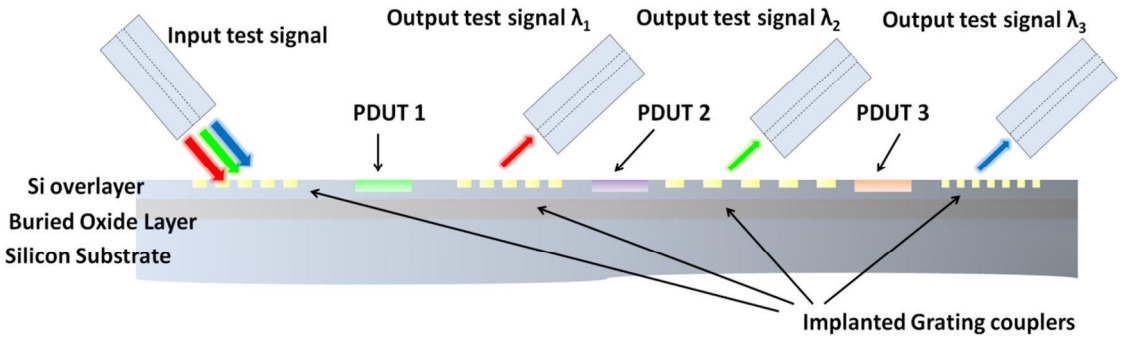

Fig. 4: Schematic of a testing configuration in which 3 devices are tested at different wavelengths via broad and/or narrow band grating couplers. The couplers would subsequently be erased.

The erasable coupler devices are formed by implanting silicon waveguides with Germanium ions, in a periodic structure to form the gratings. The energy and period will be determined by the design required for the grating operation. In our work we have fabricated several example gratings in order to demonstrate proof of principle. We have utilised 220nm high silicon wire waveguides with a 400nm width to ensure single mode operation; the buried silicon dioxide layer has a thickness of 2μm. The waveguide grating width is increased to 10μm via a dual step taper to maximise the overlap integral between the fibre and waveguide grating modes, and to facilitate straightforward alignment between fibre and waveguide. The taper flare angle from 10μm to 3μm is set at 0.6° and the angle from 3μm to 400nm at 0.2°.

Electron beam lithography was used to pattern a resist, before the entire structure was implanted with germanium ions using a dose of 1×10^{15} ions cm^{-2} to ensure complete amorphisation. The implantation energy is varied depending on the required depth of amorphisation. After testing, the grating can be erased from the optical circuit using local laser annealing.

The gratings are therefore formed by periodic regions of amorphous and crystalline allotropes of silicon, patterned to create a modulated effective index due to differing refractive indices of each allotrope. This is because the amorphised regions exhibit a positive Δn compared with crystalline silicon regions. The refractive index change introduced by ion implantation induced lattice disorder in silicon was previously reported in, for example, [18]. The threshold level of lattice disorder required for amorphous silicon formation varies in the literature (e.g. [19-21]) with a more detailed explanation given in [22]. However, there is a good agreement when the defect density threshold for amorphisation is calculated with a defect density model, in that the crystalline – amorphous transition occurs with a critical point defect density of 1.15×10^{22} cm^{-3} [20,23]. We have demonstrated that Δn increases with an increase in dose, to a maximum Δn of approximately 0.58.

Germanium was selected as the specie to be implanted because in simulations it demonstrated the best amorphous grating profile from the species simulated. Germanium offers low lateral straggling and also achieves amorphisation with a relatively low dose. Selecting a CMOS compatible element as the ion specie also has benefits in the increased ease of process adoption. The amount of disorder accumulated in the lattice is strongly dependant on the sample temperature and implanted dose as well as the implanted ion mass. The dose used in this work was 1×10^{15} ions cm^{-2} and implants were performed at room temperature with a beam current of 6.5μA. The devices were testing using the structure of figure 5(a). This enables the erasable gratings to be compared to conventional etched gratings as well as showing how after annealing the light passes though implanted grating rather than outcoupling. Figure 5(b) shows the change in throughput before and after grating erasing. The difference in the two curves is approximately 6dB, suggesting that prior to erasing, the implanted coupler picks off the signal. In separate measurements, we demonstrate output from the implanted grating to vary by approximately 21dB before and after annealing.

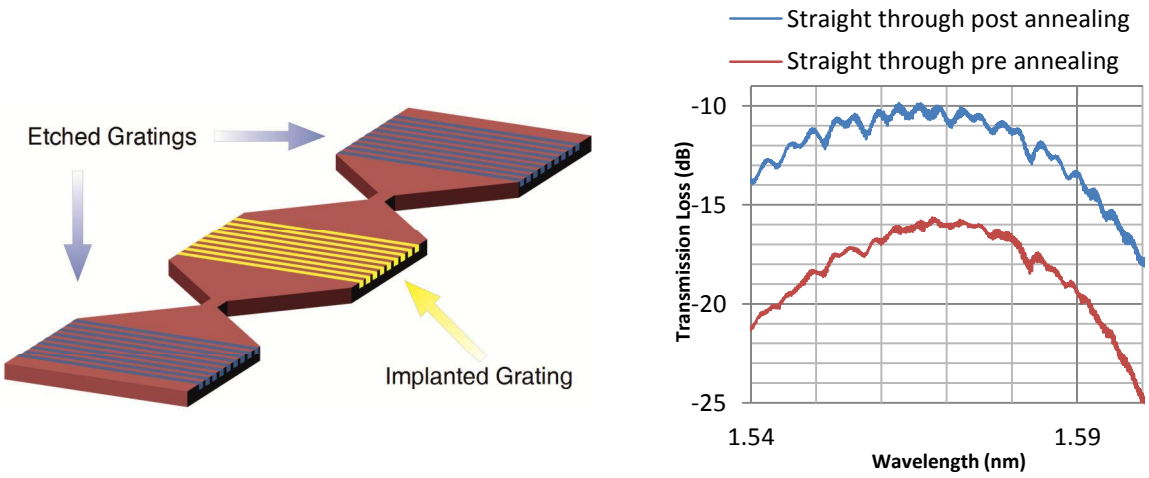

(a) (b)

Fig 5: Bow tie structure for characterising erasable gratings (a) and throughput between etched gratings before and after annealing of the erasable couplers (b)

MID IR BUILDING BLOCKS

In this section we present some examples from a range of photonic components that we have recently developed to operate in the mid infrared wavelength bands.

Multimode interference splitters

Multimode interference (MMI) splitters are important devices that we have used in fast optical modulators [1] and in multiplexers [15]. Here, we report results for MMIs designed for 3.8 µm in silicon with 400nm overlayer SOI [24]. An SEM image of a fabricated device is shown in figure 6. Refering to the annotations in figure 6 the optimum design dimensions for the 400 nm structures were: WMMI = 8 µm, LMMI = 21.0 µm, S = 4.18 µm, Wtap = 2.6 µm, Ltap = 20 µm. The insertion loss was measured by cascading different numbers of pairs of MMIs together (2-18), and plotting a line of best fit between the plotted outputs as shown in figure 7. The minimum measured insertion loss per MMI was determined to be 0.10±0.01 dB at a wavelength of 3.8 µm. The loss figure achieved is of similar magnitude to the lowest reported losses for MMIs at near-infrared wavelengths [25,26] and are much lower than previously reported values in the MIR [27,28].

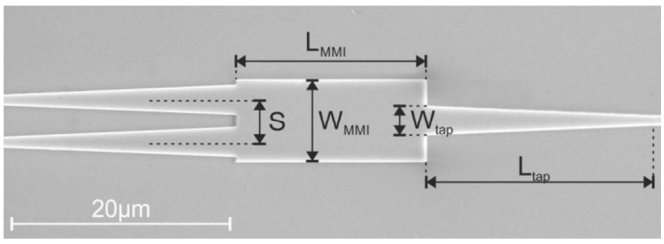

Fig. 6. SEM image of a fabricated 1×2 MIR SOI MMI with tapered input and output ports.

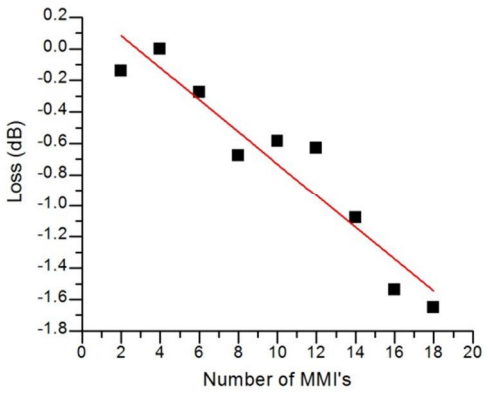

Fig. 7. Insertion loss measurement for 400 nm thick SOI MIR MMIs.

Slot waveguides

For increased sensitivity of future MIR silicon photonic sensors, a slot waveguide can be used as it can enhance the electric fields amplitude in the gap region (up to 20× higher) as compared to standard waveguide structures. We have fabricated and characterised the properties of slot waveguides for the 3.8um wavelength band [24]. Coupling to the slot waveguide was achieved by first coupling to conventional rib waveguides using grating couplers and then using a rib-slot transition as shown in figure 8.

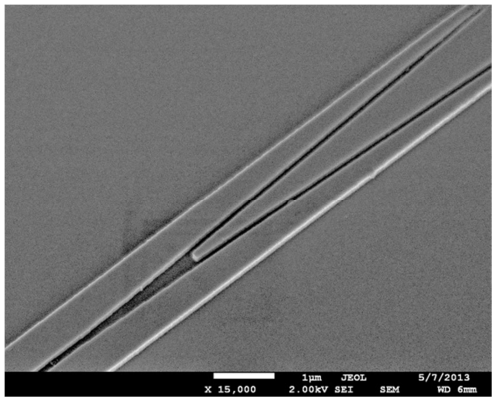

Fig. 8. SEM image of a rib-slot waveguide interface.

The devices were fabricated on 6-inch SOI wafers with 400 nm Si on 2 µm BOX using e-beam lithography and ICP etching. The slot width, the gap in the interface region, and the length of slot waveguides were varied. The rib and slot waveguides, as well as the grating couplers were fabricated with a 220 nm etch depth, hence the entire fabrication process was performed by a single etch step. By cascading different numbers of pairs of rib-slot transitions and plotting a line of best fit between the plotted outputs, we determined that a 100 nm gap in the rib-slot transition showed a loss of 0.04 dB/interface, whilst the loss was 0.06 dB/interface for a gap of 130 nm. The propagation loss for slot waveguides with the total width of 1.42 µm and slot width of 100-140 nm was 9-10 dB/cm. Reduction of the propagation loss can be achieved by designing slightly wider waveguides, smoothing the sidewalls and by a further reduction of the gap.

Mach-Zehnder interferometers

Mach-Zehnder interferometers (MZIs) are commonly used in silicon photonics as a key building block of modulators [1,2,4-11], and are also used as wavelength filters. We have fabricated asymmetric MZIs with one input and one output,

with MMIs used as splitters and couplers [24]. In devices with both 400 nm and 500 nm thick Si layers the total MZI length of the shorter arm was 928 μm, and the arm length differences were 300 μm and 350 μm, respectively. The transmission spectra were normalized to that of a standard waveguide. The measured insertion loss over the 3.7-3.9 μm wavelength range was 1.6-2.4 dB, the maximum extinction ratio was between 27 dB and 34 dB, and the FSR around 10 nm.

Here, we also report a MIR MZI based on slot waveguides, a structure that can be interesting for sensing applications. Fig. 9 shows the response from an asymmetric MZI with an arm length difference of 350 μm, and with a straight slot waveguide section 585 μm long. The rib-slot interface gap was 130 nm. It is worth noting that because of the mode-hopping behavior of the commercial QCL used for these measurements it is difficult to interrogate fine wavelength features, and some of the peaks in the spectra appear to have multiple minima or were clipped.

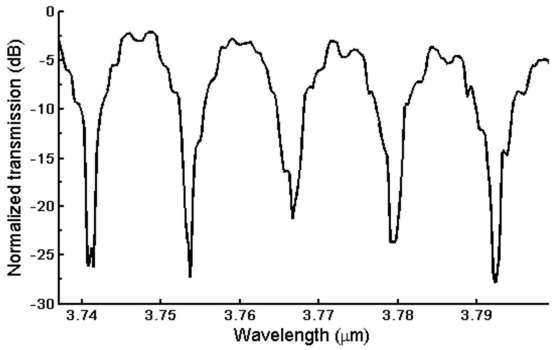

Fig. 9. Response of a Mach-Zehnder asymmetric interferometer based on slot waveguides.

Multiplexer

Multiplexers/demultiplexers are important photonic devices for future MIR high-speed datacom/telecom integrated circuits and sensors. We have demonstrated a 3 channel angled MMI based multiplexer operating in the mid infrared wavelength bands [24]. The width of the input and output waveguides was 28um whichlt the width of the multimode waveguide was 50um. The length between the input waveguide and output waveguides was 5132um, 5066um and 5000um. Refering to figure 2 θ_t in this case was 26.4°.

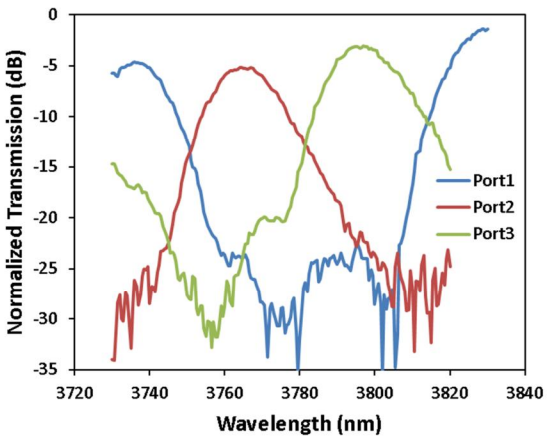

Fig. 10. Experimental response of a 3-channel MIR angled MMI.

The measured spectral response of the fabricated device is shown in Fig. 10, which has a channel spacing of 30 nm, an insertion loss of about 4-5 dB and a cross talk of –12 dB. The measured data is subject to the stability of the MIR laser source. Whilst these values are slightly higher than those demonstrated in the NIR, one can see that the merits of the AMMI structure for WDM in the NIR wavelength range, e.g. low insertion loss and low cross-talk are maintained around the wavelength of 3.8 μm.

SUMMARY

In this paper we have demonstrated some example results of our recent work on silicon photonics. Active MZI based modulators operating up to 50Gbit/s have been demonstrated as well as the integration of these modulators with drive electronics and other photonic components. A novel multiplexing structure based upon an angled MMI structure has been demonstrated with 4 and 8 channels. A new attractive approach for wafer scale testing which allows for temperorary grating coupler test points to be formed and erased is demonstated. Finally some examples from a library of MID IR based photonic components that we have been developing has been demonstrated.

REFERENCES

[1] - D. J. Thomson, F. Y. Gardes, Y. Hu, G. Mashanovich, M. Fournier, P. Grosse, J-M. Fedeli and G. T. Reed, "High contrast 40Gbit/s optical modulation in silicon," Optics Express, 19(12), pp. 11507 – 11516, 2011.

[2] - F. Y. Gardes, D. J. Thomson, N. G. Emerson, and G. T. Reed, "40 Gb/s silicon photonics modulator for TE and TM polarisations," Optics Express, 19(12), pp. 11804-11814, 2011.

[3] - D. J. Thomson, F. Y. Gardes, D. C. Cox, J-M. Fedeli, G. Z. Mashanovich, and G. T. Reed, "Self-aligned silicon ring resonator optical modulator with focused ion beam error correction," Journal of Optical Society of America B, vol. 30(2), pp. 445-449, 2013.

[4] - A. Brimont, D. J. Thomson, F.Y. Gardes, J. M. Fedeli, G. T. Reed, J. Martí, P. Sanchis, "High contrast 40 Gb/s operation of a 500 μm-long silicon carrier depletion slow wave modulator," Optics Letters, vol. 37, pp. 3504-3506, 2012.

[5] - A. Brimont, A. M. Gutierrez, M. Aamer, D. J. Thomson, F. Y. Gardes, J.-M. Fedeli, G. T. Reed, J. Martí, and P. Sanchis, "Slow light enhanced silicon optical modulators under low drive voltage operation," IEEE Photonics Journal, vol. 4, pp. 1306–1315, 2012.

[6] - A. Brimont, D. J. Thomson, P. Sanchis, J. Herrera, F. Y. Gardes, J. M. Fedeli, G. T. Reed, and J. Marti, "High speed silicon electro-optical modulators enhanced via slow light propagation," Optics Express, vol. 19, pp. 20876-20885, 2011.

[7] - D. J. Thomson, F. Y. Gardes, J-M. Fedeli, S. Zlatanovic, Y. Hu, B. P. P. Kuo, E. Myslivets, N. Alic, S. Radic, G. Z. Mashanovich, and G. T. Reed, "50-Gb/s silicon optical modulator," IEEE Photonics Technology Letters 24(4), pp. 234-236, 2012.

[8] - M. Aamer, D. J. Thomson, A. M. Gutierrez, A. Brimont, F. Y. Gardes, G. T. Reed, Jean-Marc Fedeli, A. Hakansson, and P. Sanchis, "10Gbit/s error-free DPSK link using a push-pull dual-drive silicon modulator," Optics Communications, vol. 304, pp. 107-110, 2013.

[9] - D. J. Thomson, F. Y. Gardes, Y. Hu, G. Mashanovich, G. T. Reed, L. Zimmermann, D. Knoll, S. Lischke, H. Porte, B. Goll, H. Zimmermann, L. Ke, P. Wilson, S-W. Chen, S. S. H. Hsu, G.-H. Duan, A. Le Liepvre, C. Jany, A. Accard, M. Lamponi, D. Make, F. Lelarge, S. Messaoudene, D. Bordel, J.-M. Fedeli, S. Keyvaninia, G. Roelkens and D. Van Thourhout, "Integration of high performance silicon optical modulators," IEEE Group IV Photonics, Seoul, Korea, 28-30 August 2013.

[10] - D. J. Thomson, H. Porte, B. Goll, D. Knoll, S. Lischke, F. Y. Gardes, Y. Hu, G. T. Reed, H. Zimmermann, L. Zimmermann, "Silicon carrier depletion modulator with 10Gbit/s driver realized in high-performance photonic BiCMOS," Laser & Photonics Reviews, DOI: 10.1002/lpor.201300116, 2013.

[11] - G.-H. Duan, C. Jany, A. Le Liepvre, M. Lamponi, A.Accard, F. Poingt, D. Make, F. Lelarge, S. Messaoudene, D. Bordel, J.-M. Fedeli , S. Keyvaninia, G. Roelkens, D. Van Thourhout, D. J. Thomson, F. Y. Gardes and G. T. Reed, "Integrated hybrid III-V/Si laser and transmitter", IPRM 2012, UCSB, Santa Barbara, CA, USA, 27-30 August 2012.

[12] - Bogaerts, W., Dumon, P., Van Thourhout, D., Taillaert, D., Jaenen, P., Wouters, J., Beckx, S., Wiaux, V., and Baets, R. G., "Compact Wavelength-Selective Functions in Silicon-on-Insulator Photonic Wires," IEEE J. Sel. Top. Quant. Electron. 12, 1394-1401 (2006).

[13] - Brouckaert, J., Bogaerts, W., Dumon, P., Van Thourhout, D., and Baets, R., "Planar concave grating demultiplexer fabricated on a nanophotonic silicon-on-insulator platform," J. Lightwave Technol. 25, 1269-1275 (2007).

[14] - Y. Hu, R. M. Jenkins, F. Y. Gardes, E. D. Finlayson, G. Z. Mashanovich, and G. T. Reed, "Wavelength division (de)multiplexing based on waveguide mode dispersion," Optics Letters, vol. 36, pp. 4488-4490, 2011.

[15] - Y. Hu, F. Y. Gardes, D. J. Thomson, G. Z. Mashanovich, and G. T. Reed, "Coarse wavelength division (de)multiplexer using interleaved angled multimode interferometer structure," Applied Physics Letters, vol. 102, 251116, 2013.

[16] - T. Baehr-Jones, R. Ding, A. Ayazi, T. Pinguet, M. Streshinsky, N. Harris, J. Li, L. He, M. Gould, Y. Zhang, A. E.-J. Lim, T.-Y. Liow, S. H.-G. Teo, G.-Q. Lo, and M. Hochberg, "A 25 Gb/s silicon photonics platform," arXiv:1203.0767 (2012).

[17] - S. Scheerlinck, et al., "Flexible metal grating based optical fiber probe for photonic integrated circuits," Applied Physics Letters, vol. 92, pp. 031104-3, 2008.

[18] - E. Baranova, V. Gusev, W. Martynenko, C. Starinin, and I. Haibullin, "On silicon amorphization during different mass ion implantation," Radiation Effects 18, 21-26 (1973).

[19] - L. A. Christel, J. F. Gibbons, and T. W. Sigmon, "Displacement criterion for amorphization of silicon during ion implantation," Journal of Applied Physics 52, 7143-7146 (1981).

[20] - H. Cerva, and G. Hobler, "Comparison of Transmission Electron Microscope Cross Sections of Amorphous Regions in Ion Implanted Silicon with Point-Defect Density Calculations," Journal of The Electrochemical Society 139, 3631-3638 (1992).

[21] - J. R. Dennis, and E. B. Hale, "Crystalline to amorphous transformation in ion-implanted silicon: a composite model," Journal of Applied Physics 49, 1119-1127 (1978).

[22] - G. Hobler, and G. Otto, "Status and open problems in modeling of as-implanted damage in silicon," Materials Science in Semiconductor Processing 6, 1-14 (2003).

[23] - O. Engström, S. Bengtsson, G. I. Andersson, M. O. Andersson, and A. Jauhiainen, "Electrical characterization of bonding interfaces," Journal of The Electrochemical Society 139, 3638-3644 (1992).

[24] - M. Nedeljkovic, A. Z. Khokhar, Y. Hu, X. Chen, J. Soler Penades, S. Stankovic, H. M. H. Chong, D. J. Thomson, F. Y. Gardes, G. T. Reed, and G. Z. Mashanovich, "Silicon photonic devices and platforms for the mid-infrared," Optical Materials Express, vol. 3, pp. 1205–1214, (2013).

[25] - D. J. Thomson, Y. Hu, G. T. Reed, and J.-M. Fedeli, “Low loss MMI couplers for high performance MZI modulators,” IEEE Photon. Technol. Letters 22, 1485-1487 (2010).

[26] - W. Bogaerts, S. K. Selvaraja, P. Dumon, J. Brouckaert, K. De Vos, D. Van Thourhout, and R. Baets, “Silicon-on-insulator spectral filters fabricated with CMOS technology,” IEEE J. Sel. Top. Quant. 16, 33-44 (2010).

[27] - M. M. Milosevic, M. Nedeljkovic, T.-B. Masaud, E. Jaberansary, H. M. H. Chong, N. G. Emerson, G. T. Reed, and G. Z. Mashanovich, “Silicon waveguides and devices for the mid-infrared,” Appl. Phys. Lett. 101, 121105 (2012).

[28] - Y. Wei, G. Li, Y. Hao, Y. Li, J. Yang, M. Wang, and X. Jiang, “Long-wave infrared 1 × 2 MMI based on air-gap beneath silicon rib waveguides,” Opt. Express 19, 15803-15809, (2011).